Hindawi
Geofluids
Volume 2017, Article ID 4580416, 15 pages
https://doi.org/10.1155/2017/4580416

Research Article

Distribution and Thermal Maturity of Devonian Carbonate Reservoir Solid Bitumen in Desheng Area of Guizhong Depression, South China

Yuguang Hou,[1] Yaqi Liang,[1,2] Sheng He,[1] Yukun Liu,[1] Zhiwei Fan,[3] and Yingrui Song[1]

[1]*China University of Geosciences Key Laboratory of Tectonics and Petroleum Resources, Ministry of Education, Wuhan 430074, China*
[2]*Geological Experimental Testing Center of Hubei Province, Wuhan 430034, China*
[3]*Petroleum Exploration Branch Company, Sinopec, Chengdu 610041, China*

Correspondence should be addressed to Yuguang Hou; sporthyg@126.com and Sheng He; shenghe@cug.edu.cn

Received 3 March 2017; Revised 18 May 2017; Accepted 28 June 2017; Published 15 August 2017

Academic Editor: John A. Mavrogenes

The distribution of solid bitumen in the Devonian carbonate reservoir from well Desheng 1, Guizhong Depression, was investigated by optical microscope and hydrocarbon inclusions analysis. Vb and chemical structure indexes measured by bitumen reflectance, laser Raman microprobe (LRM), and Fourier transform infrared spectroscopy (FTIR) were carried out to determine the thermal maturity of solid bitumen. Based on the solid bitumen thermal maturity, the burial and thermal maturity history of Devonian carbonate reservoir were reconstructed by basin modeling. The results indicate that the fractures and fracture-related dissolution pores are the main storage space for the solid bitumen. The equivalent vitrinite reflectance of solid bitumen ranges from 3.42% to 4.43% converted by Vb (%) and LRM. The infrared spectroscopy analysis suggests that there are no aliphatic chains detected in the solid bitumen which is rich in aromatics C=C chains (1431–1440 cm^{-1}). The results of Vb (%), LRM, and FTIR analysis demonstrate that the solid bitumen has experienced high temperature and evolved to the residual carbonaceous stage. The thermal evolution of Devonian reservoirs had experienced four stages. The Devonian reservoirs reached the highest reservoir temperature 210–260°C during the second rapid burial-warming stage, which is the main period for the solid bitumen formation.

1. Introduction

Reservoir bitumen, a type of solid and amorphous organic matter, is the product of maturation of organic matter and can be regarded as a critical symbol to prospect hydrocarbon reservoirs [1–5]. The origin of reservoir solid bitumen is generally attributed to thermal cracking and nonthermal cracking. The thermal events, such as the high overburden temperature and the activity of igneous rocks, can generate the thermal gradual change bitumen and the thermal spikes bitumen, respectively [6]. In the high temperature geothermal-system, the light component chains of bitumen are eventually alkanoylated to generate methane, and the heavy component is condensed to form a polycyclic coke bitumen residue characterized by a high carbon compound. The pyrolytic bitumen represents the end product of oil thermal cracking. The accumulation of pyrolytic bitumen in reservoirs usually can be used to indicate industrial oil-gas reservoirs. The formation of nonthermal cracking reservoir bitumen is basically due to oxidation, biodegradation, water washing, and deasphalting. Biodegradation is thought to be the most common trigger to secondary alteration of hydrocarbon and accounts for most of heavy oil in the world [7–9].

The occurrence state and geochemical characteristics of solid bitumen record the processes of hydrocarbon generation, migration, and accumulation. There is abundant geological information which is useful for exploration and

exploitation activities in oil and gas bearing basin. The formation and evolution of bitumen are closely related to the evolution history of oil-gas reservoirs, which are of great significance to understand the history of oil and gas reservoirs formation, reconstruction, and destruction [10–12].

Determination of the thermal maturity of solid bitumen is very important to reconstruct the evolution history of reservoirs. Comparing with the bitumen reflectance detection, the laser Raman microprobe (LRM) and Fourier transform infrared spectroscopy (FTIR) can provide maturity information from the chemical structure of solid bitumen. Depending on the ordering degree of the molecular structure arrangement and the change of chemical composition during the thermal evolution, the Raman spectrum characteristic peaks of carbonaceous organic matter show a systematic change with the increase of maturity. Therefore, it can be used as an indicator of Raman spectroscopy that reflects the maturity of carbonaceous organic matter [13, 14]. The correlation between the parameters of laser Raman spectroscopy and the vitrinite reflectance of organic carbonaceous matter has been studied, and several corresponding regression relationships have been proposed [15–18]. Infrared spectroscopy is proven to be an effective method in determining the structure and composition of hydrocarbon organic matter [19, 20]. With increasing maturity, the change of functional groups on FTIR corresponds to the chemical structure conversion of organic matter. During the process of thermal evolution, the aliphatic bands are gradually reduced, to vanish eventually. However, the absorption band of aromatic hydrocarbon will correspondingly increase.

Guizhong Depression is one of the most important areas for oil and gas exploration in the marine carbonate rocks, southern China [21–24]. It is characterized by complex tectonic evolution, multiple sedimentary systems, and multistage hydrocarbon accumulations. Abundant oil-gas seepages in the Guizhong Depression including 31 oil-gas seepages and 57 bitumen displays (32 of Devonian, 35 of Carboniferous, 15 of Permian, and 6 of Triassic) have been found previously [25]. The abundant reservoir bitumen and oil sands not only indicate the history of large-scale hydrocarbon generation, migration, and accumulation in this area but also imply the complexity and risk for oil and gas exploration in this area. After having experience of oil and gas exploration in this area for more than 40 years, it is generally accepted that this area has the primitive geological conditions for the formation of medium to large size oil-gas field. Although the ancient reservoirs have undergone frequent destruction and alteration, they may still have residual reservoirs [22, 23, 26].

In 2014, Sinopec deployed the deepest prospecting well Desheng-1 (in what follows named as DS1) on the Desheng biohermal lithologic traps in the Yishan fault depression, north of Guizhong Depression. The drilling depth of well DS1 was 5170.00 m, and its target drilling stratigraphic unit was the Lower Devonian Yujiang Formation. There are no obvious oil and gas shows in the target layer, but some reservoir bitumen shows were found in the Devonian carbonate reservoir. The major objectives of this study were to (1) investigate the distribution characteristics of solid bitumen in the Devonian carbonate reservoir of well DS1 by physical property observation; (2) document the thermal maturity of the reservoir solid bitumen by reflectivity detection and chemical structure indexes analysis; (3) reconstruct the burial and thermal maturity history of bituminous reservoir based on the erosion thickness restoration and basin modeling technique. Our results not only have theoretical significance but also provide scientific guidance to oil and gas assessment, strategic area selection, and exploration deployment in the study area.

2. Geological Setting

The Guizhong Depression is located at the junction zone between the southern margin of the Yangtze plate and the southern Caledonian fold belt (Figure 1(a)). The Guizhong Depression, covering approximately $4.6 \times 10^4\,km^2$ is an important part of the Nanpanjiang-Youjiang Basin [21, 27, 28]. This depression can be further divided into 13 subtectonic units. The study area is located in the Yishan fault sag of the Guizhong Depression (Figure 1(b)).

The Guizhong Depression is a large Late Paleozoic marine sedimentary depression overlying the Caledonian movement, which is mainly composed of the Upper Paleozoic marine strata (Figure 2) [30]. During the Hercynian period ($D - P_1$), the study area gradually entered the passive continental margin depression stage. The sedimentary thickness from Devonian to Early Permian is more than 14,000 m [23, 31]. The Lower Devonian was deposited in the tidal flat-shore environment. During Middle and Late Devonian stage, this depression was mainly filled with carbonate and mudstone deposits, formed in the platform and interplatform environment. The Middle and Late Devonian was the main period of reef development [26, 32]. After a brief erosion of the Dongwu movement, the study area entered the Indosinian period. Thick layer of clastic rocks was deposited from the Late Permian to Middle Triassic in the study area [24]. By the late stage of Middle Triassic, the marine sedimentary history of the study area came to an end due to the basin-mountain transition. During the Yanshan-Himalayan period, the Guizhong Depression suffered continuous extrusion uplift. There is less deposition of Triassic-Cretaceous deposit retained by synclines in this study area, and the thickness is about 1500 m [33].

The hydrocarbon accumulation condition of Guizhong Depression was superior in the geological history [22]. The residual bitumen stored in the famous Middle Devonian paleoreservoir of Dachang reef is estimated to be tens of millions of tons. Previous studies suggest that the original oil accumulation could be more than 100 million tons [22, 24]. Therefore, the Devonian is the main target strata for the oil and gas exploration in the study area (Figures 2 and 3). The mudstone of the Middle Devonian Tangding Formation and Luofu Formation deposited in the interplatform basin are the main source rocks, and the dolomite and biohermal limestone deposited in the platform are the main reservoir. Both the mudstone and limestone of Upper Devonian deposited in the interplatform basin and foreslope could be the potential cap rock.

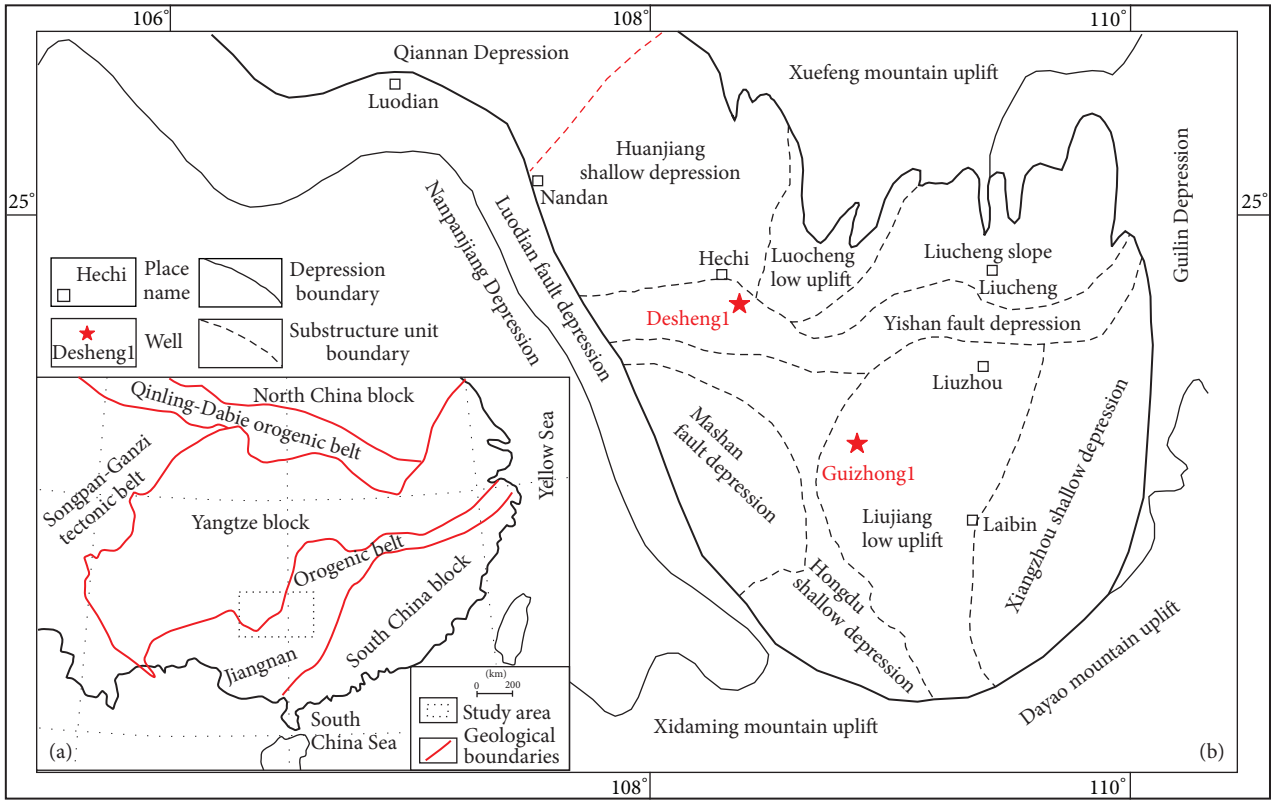

FIGURE 1: (a) The location of the Guizhong Depression. (b) The subtectonic units of Guizhong Depression and the location of sampling wells.

3. Samples and Methods

3.1. Samples. We collected carbonate samples from Upper Devonian Rongxian Formation and Middle Devonian Yingtang Formation and Donggangling Formation (Figure 2). These formations were deposited in the reef subfacies of the carbonate platform-platform edge. Yingtang Formation is comprised of algal marl and black-gray dolomite. The brachiopod fossils are distributed in the algae marlite, and the thin layer of tiny asphalt particles can be observed on the core cross-section. The 1st section of Donggangling Formation is composed of a set of black-gray algae marl. Rongxian formation developed the oolitic limestone and algal mudstone, and gray-black sheet of highly evolved bitumen can be seen on their core cross-section. Porosity types of the carbonate reservoir can be divided into intraparticle pore and interparticle pore within ooids, intergranular pore within dolomite, dissolution pore and cave, microfracture, and so forth.

In this study, reservoir solid bitumen observation and hydrocarbon inclusions detection were carried out on the carbonate reservoir samples. The laser Raman microprobe analysis was used to determine the composition of the bitumen and hydrocarbon inclusions. The bitumen reflectance detection, laser Raman microprobe, and Fourier transform infrared spectroscopy (FTIR) were used to determine the thermal maturity of solid bitumen. The burial and thermal maturity history of carbonate reservoir bearing solid bitumen of well DS1 were reconstructed by using Basin Model Simulation Software. FTIR analysis was performed at the Materials and Chemical Analysis and Testing Center, China University of Geosciences (Wuhan). All the other tests were completed at the Key Laboratory of Structural and Oil and Gas Resources, Ministry of Education, China University of Geosciences (Wuhan).

3.2. Identification on Solid Bitumen and Hydrocarbon Inclusions. 15 carbonate samples were selected to make the casting thin section slides. The distribution characteristics of solid bitumen and pore structure in these carbonate rocks were studied by using the transmission microscope of Nikon Eclipse LV100 POL, 5x (+). The surface porosity (within bitumen or not) was also be estimated.

Six carbonate samples and 13 calcite vein samples were selected to make double-side polishing thin sections and were analyzed on the identification of hydrocarbon inclusions by using Nikon Eclipse LV100N POL, 100x (+).

3.3. Laser Raman Microprobe Analysis. The composition of solid bitumen and hydrocarbon inclusions were analyzed by the laser Raman spectroscopy. The Raman microprobe analyses were collected with a JY/Horiba LabRam HR800 Raman system at room temperature of 25°C, equipped with a frequency doubled Nd:YAG laser (532.06 nm) where output laser power is 14 mW, and laser hit the surface of the sample power is generally 2~12 mW with the line width <0.1 nm. It was equipped with a 50x long-work-distance Olympus

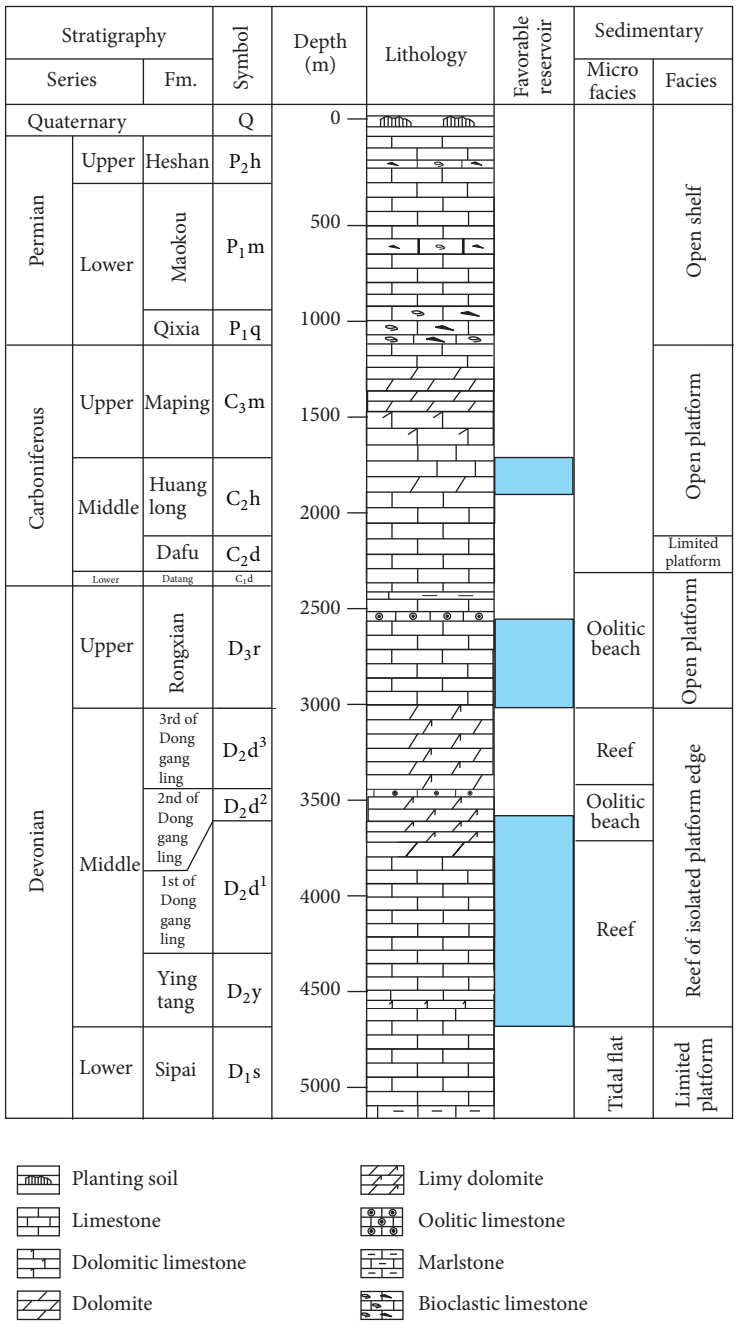

Figure 2: The stratigraphic framework of well DS1, Guizhong Depression (see well location in Figure 1).

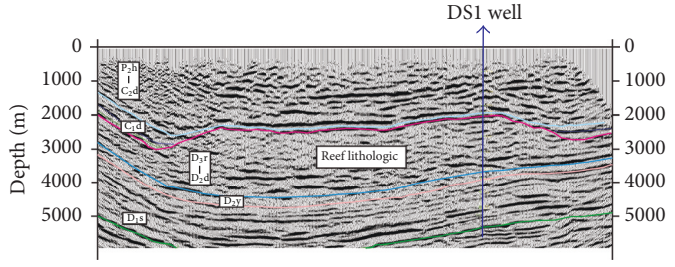

Figure 3: Seismic profile of reef lithologic at Desheng area (strata correspond to Figure 2).

objective with a numerical aperture of 0.5. The aperture of the confocal hole was set to 200 μm. Raman peak position was regularly calibrated with the ~520.7 cm^{-1} band of a polished silicon wafer. The spatial resolution was 0.1 μm in the transverse direction and 0.3 μm in the longitudinal direction, and the data was collected every 40 seconds.

3.4. Bitumen Reflectance Analysis. Limited by the sample weight of the test required, only two solid bitumen samples from 1st section of Upper Devonian Donggangling Formation were selected for bitumen reflectance analysis. Jacob [34] proposed that bitumen reflectance could be used as a maturity parameter, due to the stochastic linear relationship between the reflectances of vitrinite and bitumen. Several conversion formulas between the bitumen reflectance and the vitrinite were summarized by Jacob [34], Feng and Chen [35], and Liu and Shi [36]:

$$\begin{aligned} R_o &= 0.6180R_b + 0.4000 \quad [34], \\ R_o &= 0.6790R_b + 0.3195 \\ &\qquad \text{base on pyrolysis simulation experiment } [35], \\ R_o &= 0.6569R_b + 0.3364 \\ &\qquad \text{base on natural thermal evolution } [35], \\ R_o &= 0.6880R_b + 0.3460 \quad [36], \end{aligned} \tag{1}$$

where R_o is the vitrinite reflectance and R_b the bitumen reflectance.

Thermal maturity of the two solid bitumen samples was determined by measuring bitumen reflectance and then converting into the vitrinite reflectance by using the above equations.

3.5. Fourier Transform Infrared (FTIR) Spectroscopy Analysis. The solid bitumen samples from Upper Devonian Rongxian Formation were analyzed by FTIR. Prior to the experiment, 2 g of the bitumen powder sample was placed in a low-temperature drying oven and dried less than 80°C. Samples were fully mixed with potassium bromide in a ratio of 1 : 150, and then we placed the mixture in tablet press tested by Thermo Infrared spectrometer. The test is based on GB/T6040-2002 with the detection-ambient temperature of 23°C and the relative humidity of 53%. The infrared spectrum of the bitumen organic matter is in the range of 4000~400 cm^{-1}.

3.6. Basin Modeling. One-dimensional modeling technology can be used to simulate hydrocarbon generation and primary migration, defined as movement of hydrocarbon through and out of the source rocks [37]. BasinMod software was used to carry out the one-dimensional modeling of burial and thermal maturity history. According to the geological background of the study area and conceptual model [15], the instantaneous heat flow history model and the EASY% *Ro* mature history model are used to simulate the thermal evolution history of well DS1. The equivalent reflectivity of bitumen and inclusions was used to calibrate modeling results in this study [38, 39].

4. Results

4.1. Distribution Characteristics of Solid Bitumen. Thin section analysis suggests that the solid bitumen is mainly concentrated in the Upper Devonian Rongxian Formation (2860 m–2870 m), Middle Devonian Donggangling Formation (4210 m–4220 m), and the Yingtang Formation (4640 m–4655 m). The surface porosity filled with solid bitumen ranges from 3% to 8% and is slightly higher in the Rongxian Formation.

Three main filling types of solid bitumen in the reservoir have been observed: fracture filling, dissolution pore filling, and recrystallization pore filling.

Fracture Filling. This filling type is mainly developed in the limestone reservoirs. According to the characteristics of fractures filled with solid bitumen, the fractures can be divided into two types: structural fractures and diagenetic dissolution fractures. Structural fractures are mainly found in oolitic limestone of the Upper Devonian Rongxian Formation (Figure 4(a)). The combination of main fracture with branch fractures has the shear characteristics and is distributed in the form of horsetail. The morphology of the ooids on the two sides of the fractures is quite different. The surrounding ooids were always cut through by the fractures, and the broken ooids were filled or disseminated by the bitumen (Figure 4(b)). Diagenetic dissolution fractures display bending and irregular shape and are commonly found in the limestone reservoirs of all layers (Figures 4(c)–4(f)). In the algae marl of the Middle Devonian Donggangling Formation, these fractures are developed around large blocks of calcite crystals (Figures 4(c) and 4(d)). In the black-gray limestone and algae marl of the Middle Devonian Yingtang Formation, it was shown that different fractures filling bitumen interpenetrated each other (Figures 4(e) and 4(f)). This type of fracture is generally filled with bitumen and a small amount of microcrystalline calcite or fine-grained calcite.

Dissolution Pore Filling. This filling type of solid bitumen is mainly distributed in the oolitic limestones of the Upper Devonian Rongxian Formation. The dissolution pores of ooids filled with solid bitumen are commonly distributed around the microfractures (Figure 4(a)). The ooids close to the fractures are inclined to be disseminated be by bitumen, but the ooids far away from the fractures are well preserved. The solid bitumen within the dissolved ooids displays flocculent and pure black. The filling substance between ooids is mainly composed of microcrystalline calcite or fine-grained calcite. The calcite crystals that are large in size and well-crystallized can be seen occasionally but are not affected by bitumen. In the Donggangling Formation, a small amount of dissolution pore is distributed around the dissolution fractures, and the pores have been filled with carbonaceous bitumen (Figure 4(c)).

Recrystallization Pore Filling. They are mainly distributed in dolomitic limestones of the Middle Devonian Yingtang

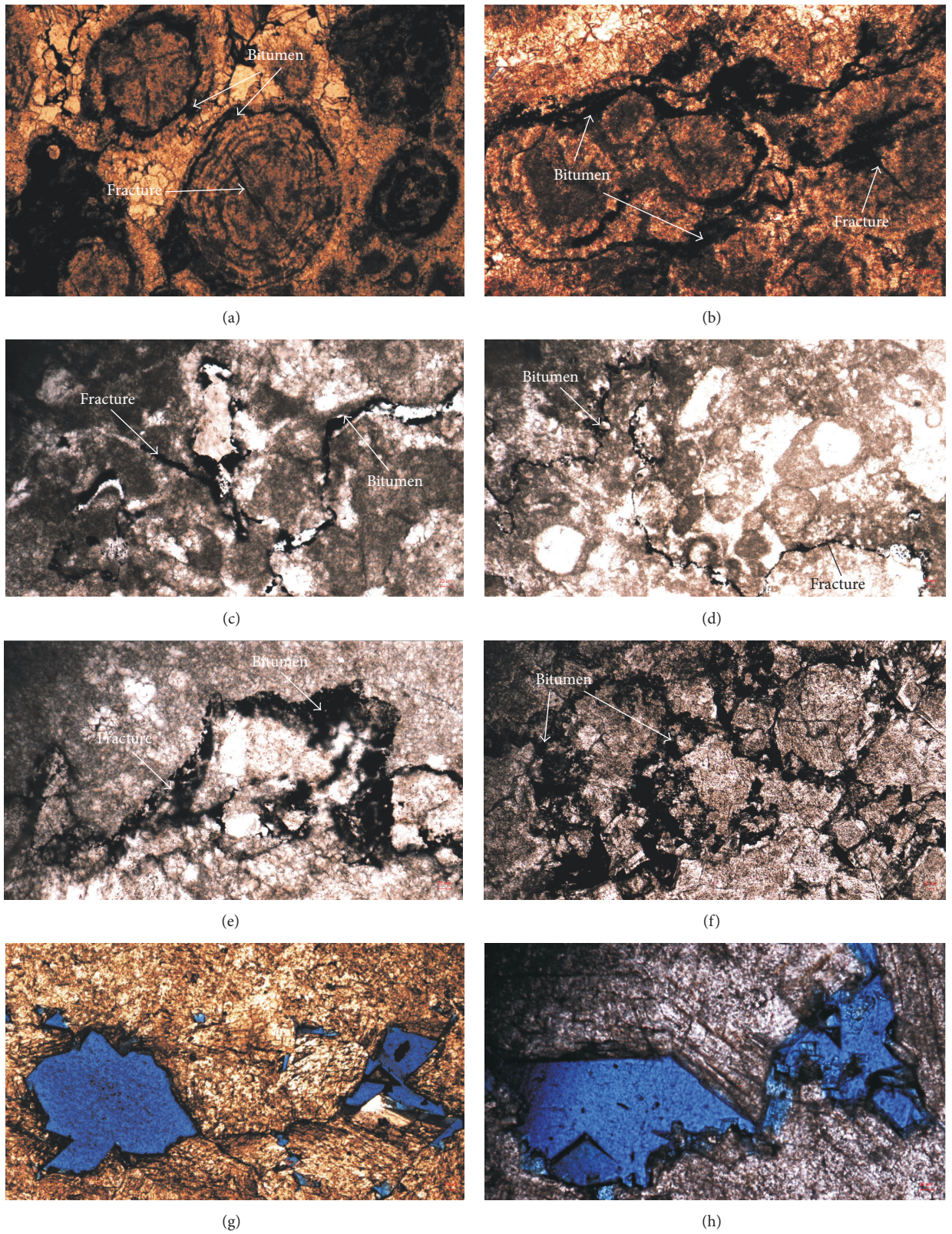

Figure 4: Distribution of bitumen in the carbonate reservoirs of well DS1 in Guizhong Depression. ((a) and (b)) DS-X06, 2864.44–2864.49 m, oolitic limestones, 5x (−). Bitumen filled in the fractures and dissolved pores in Rongxian Formation. (c) DS-X44, 4211.21 m, algal mudstone, 10x (−) and (d) DS-X44, 4211.21 m, algal mudstone, 20x (−). Dissolution fractures are filled with bitumen and sparry calcite in the 1st section of Dongangling Formation. (e) DS-X51, 4648.27 m, algal mudstone, 5x (−), and (f) DS-X53, 4648.76–4648.81 m, dolomite, 5x (−). Dissolution fractures are filled with bitumen in Yingtang Formation. (g) DS-X16, 3889.97–3890.05 m, dolomite, 5x (−), and (h) DS-X19, 3894.05–3894.09 m, dolomite, 5x (−), no bitumen filled in the pores and fractures in the upper 1st section of Dongangling Formation.

Formation. The dolomitic limestone shows well-developed and well-crystallized calcite crystals. The recrystallization pores are distributed as a network, concentrate between the calcite crystals, and completely filled with bitumen (Figure 4(f)). The edge of solid bitumen is commonly straight, and some of solid bitumen shows polygonal shape. In addition, the recrystallization pores are also well developed in the dolomite reservoir in the upper 1st section of Middle Devonian Dongganglingl Formation. However, almost no solid bitumen within these pores was observed based on the cores and casting thin sections analysis (Figures 4(g) and 4(h)). There are some straight structural fractures in the Yingtang Formation without bitumen filling and without or partially filled with secondary calcite.

4.2. Characteristics of Fluid Inclusions. Fluid inclusion analysis suggests that there are a large amount of gas-liquid two-phase salt-water inclusions observed in the carbonate reservoirs and calcite veins in the Middle Devonian Yingtang Formation and the Dongganglingl Formation (Figures 5(a) and 5(b)). Basically, these inclusions are small in size, which are generally 3–5 μm in size (the smallest is less than 3 μm and the largest is close to 9 μm). The ratio of gas to liquid in the salt-water inclusions is approximately 6–12%. They display oblong or irregular shape, occurring in small clusters along the direction of fracture or paralleling mineral joints. A small amount of bitumen inclusions and methane-containing fluid inclusions were also detected, but no fluorescent hydrocarbon inclusions were observed (Figures 5(c) and 5(d)). The solid bitumen inclusions are dark gray or black in the single polarized opaque and characterized by different size and rectangular or irregular in shape. The methane-containing fluid inclusions display isolated distribution in the dolomite and calcite veins, which were gray-black in the transmission of low transparency light, and have a wide range of shapes such as oval, rectangular, and irregular shape (Figure 5(d)).

4.3. LRM of Solid Bitumen and Hydrocarbon Inclusions. Laser Raman Microprobe is a molecular spectral microanalysis technique, and it becomes an effective method for the study of carbonaceous particles in sedimentary and metamorphic sedimentary rocks [16–18]. Based on the principle of "different substances correspond to the corresponding peak position," organic carbonaceous matters have two characteristic peaks in the frequency range of 1000 cm^{-1} to 2000 cm^{-1} on the spectra. The position of the two characteristic peaks are located from 1580 cm^{-1} to 1600 cm^{-1} and 1350 cm^{-1} to 1380 cm^{-1}, respectively. The formation of the former peak is due to the vibration of the C=C bond on the aromatic configuration plane of the molecule, and the latter is due to the defect between the disordered structure and the aromatic structural unit. The characteristic peaks of hydrocarbon gas are mainly distributed 2890–2594 cm^{-1}.

Solid Bitumen. The laser Raman Microprobe analysis indicates that the dark materials filled within the microfractures and around ooids of the Upper Devonian Rongxian Formation (Figure 6(a)), in the intergranular pores and fractures of the Middle Devonian Dongganglingl Formation (Figure 6(b)) and the reticular recrystallized pores of the Middle Devonian Yingtang Formation (Figures 6(c) and 6(d)), manifesting obvious spectral peak characteristics of organic matter. By comparing with the typical laser Raman spectra of carbonaceous bitumen and pyrobitumen reported by Liu et al. [18] (Figures 6(e) and 6(f)), these dark materials can be determined as solid bitumen.

Hydrocarbon Inclusions. The laser Raman spectra of suspected bitumen inclusions in the gray dolomite of Dongganglingl Formation are shown in Figures 7(a) and 7(b). In the spectrums of bitumen inclusions, two typical organic characteristic peaks appeared in the frequency range of 1000 cm^{-1}–2000 cm^{-1}, indicating that the inclusions contained bitumen organic matter. As the inclusions are small and not clear, the test location is mostly gas-liquid-mineral mixed phase. Therefore, the spectrums often contain the characteristic peaks of the background minerals, mainly including calcite or some other carbonate minerals. Additionally, the peaks of water can also be displayed on the spectrograms, which have larger width and lower height.

The laser Raman spectra of suspected methane-containing fluid inclusions in the dolomite reservoirs of the Dongganglingl Formation and the calcite veins of the Yingtang Formation are shown in Figures 7(c) and 7(d). The response level of the inclusions' component may be limited by the size of the inclusions and their hydrocarbon content. The positions of the Methane Raman scattering peak (V_1) in the spectrograms of the Dongganglingl Formation are mainly in the range of 2910–2945 cm^{-1} (Figure 7(c)). The reason for such a wide peak may be affected by the ethane composition that existed in the inclusion. In the Yingtang Formation (Figure 7(d)), the V_1 peak in the spectrograms has higher response where the position is around 2925.99 cm^{-1}.

4.4. Thermal Maturity of Solid Bitumen

(1) Bitumen Reflectance. Thermal maturity of solid bitumen can be determined by measuring their reflectance and converting into the vitrinite reflectance [6]. The bitumen reflectance values (% R_b) of the two samples from the 1st section of Dongganglingl Formation are 5.35% and 5.44%, respectively (Table 1). The equivalent vitrinite reflectances are ranging from 3.70% *Ro* to 4.09% *Ro* based on the different conversion formulas.

(2) Equivalent Vitrinite Reflectance by LRM. Due to the regular change of the distance between vibration peaks G and D and the ratio of their heights with the increase of maturity, Liu et al. [18] proposed that equivalent reflectance ($_{Rmc}R_o$%) converted by the Raman spectroscopy analysis parameters could be used as a maturity parameter. The equivalent reflectivity of solid bitumen can be calculated through the equation "$_{Rmc}R_o\% = 1.1659h\,(\mathrm{Dh/Gh}) + 2.7588$" (where h (Dh/Gh) is the ratio of peak height of peaks G and D), which is suitable for thermal evolution stage from overmature to granular graphitization.

Table 1: Results of equivalent vitrinite reflectance by bitumen reflectance.

Sample number	Formation	Lithology of reservoir	Bitumen reflectance (%)	Equivalent vitrinite reflectance (%)			
				Jacob, 1989	Feng and Chen, 1988		Liu and Shi, 1994
					Pyrolysis	Natural	
DS1-5-1	D_2d^1	Muddy Limestone	5.35	3.70	3.95	3.85	4.03
DS1-5-4	D_2d^1		5.44	3.76	4.01	3.91	4.09

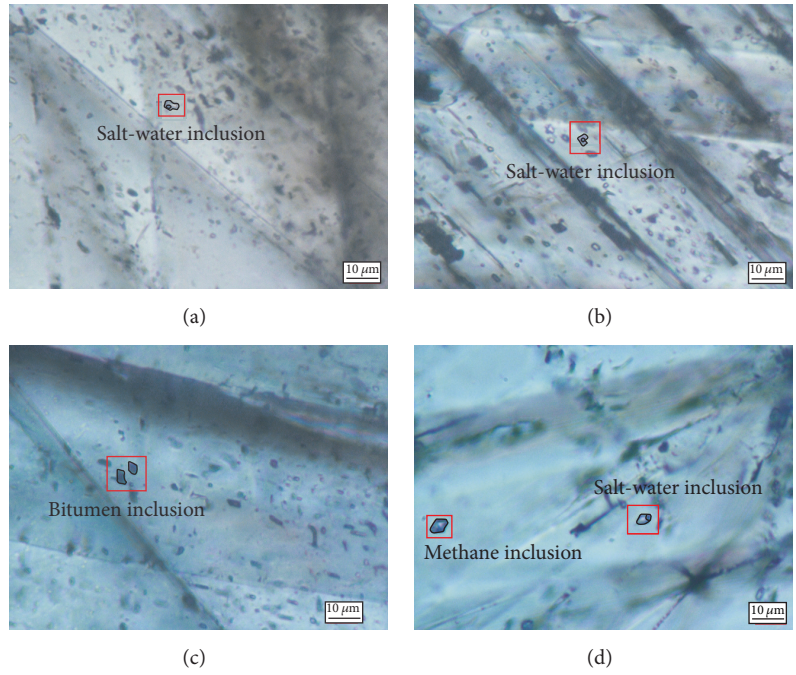

Figure 5: Photomicrographs of fluid inclusions trapped in calcite veins. ((a) and (b)) Gas-liquid two-phase salt-water inclusions in the calcite veins of carbonate reservoirs of the 1st section of Donggangling Formation, 3802.22 m, transmitted light. (c) Solid bitumen inclusions in the calcite veins of carbonate reservoirs of Yingtang Formation, 4653.16 m, transmitted light. (d) Gas-liquid two-phase salt-water inclusion and methane-containing fluid inclusion in the calcite veins of carbonate reservoirs of Yingtang Formation, 4653.16 m, transmitted light.

The equivalent vitrinite reflectance calculated from the laser Raman characteristic peaks of the bitumen in thin sections are shown in Table 2, and the values range between 3.42 and 4.43%. The equivalent vitrinite reflectance values of the bitumen inclusions range from 3.80% to 4.23% (Table 2). The conversion values are consistent with the vitrinite reflectance calculated from the measured bitumen reflectivity, and both results indicate that the Devonian carbonate reservoirs of well DS1 have experienced high thermal evolution to the quasi-metamorphism stage.

4.5. Infrared Spectroscopy of Solid Bitumen. Limited by the amount of samples, only several solid bitumen samples form the Upper Devonian Rongxian Formation are eligible for this experiment. The results are shown in Figure 8.

According to the principles of infrared spectroscopy and organic chemistry, as well as the most likely distribution of the various bands summarized by the predecessors [3, 5, 40–42], the most likely functional groups represented by the absorption peaks in the solid bitumen infrared spectrum of this test can be summarized as follows: (1) the peaks of free water, adsorbed water, crystal water, and structured water are shown, respectively, in the vicinity of 3756 cm^{-1}, 3435 cm^{-1}, 3200–3250 cm^{-1}, and 3640 cm^{-1}, which are related to stretching vibration of -OH groups in molecular water; (2) the bands locating in 1600–1550 cm^{-1} and 1450 cm^{-1} are mainly related to the C=C group skeleton vibration of aromatic hydrocarbons; (3) the bands locating in 3100–3000 cm^{-1} show the stretching vibration of the chemical bond of the C-H on the aromatic ring; (4) the absorption peak at the 1154.74–1021.46 cm^{-1} position may be related to the structure of the Si-O chemical bond of the clay mineral; (5) the weakly continuous bands at 880 cm^{-1} to 680 cm^{-1} are related to the out-of-plane bending vibration of the chemical bond of C-H of various aromatic hydrocarbons and depend on the number of adjacent protons; and (6) the bands locating in the vicinity of 1420 cm^{-1}, 955-954 cm^{-1}, and below 680 cm^{-1} are heteroatom absorption peaks.

The results show that the band peak of the oxygen-containing groups (C=O) displayed at 1710 cm^{-1} have disappeared completely (Figure 8). Only a very little band peak

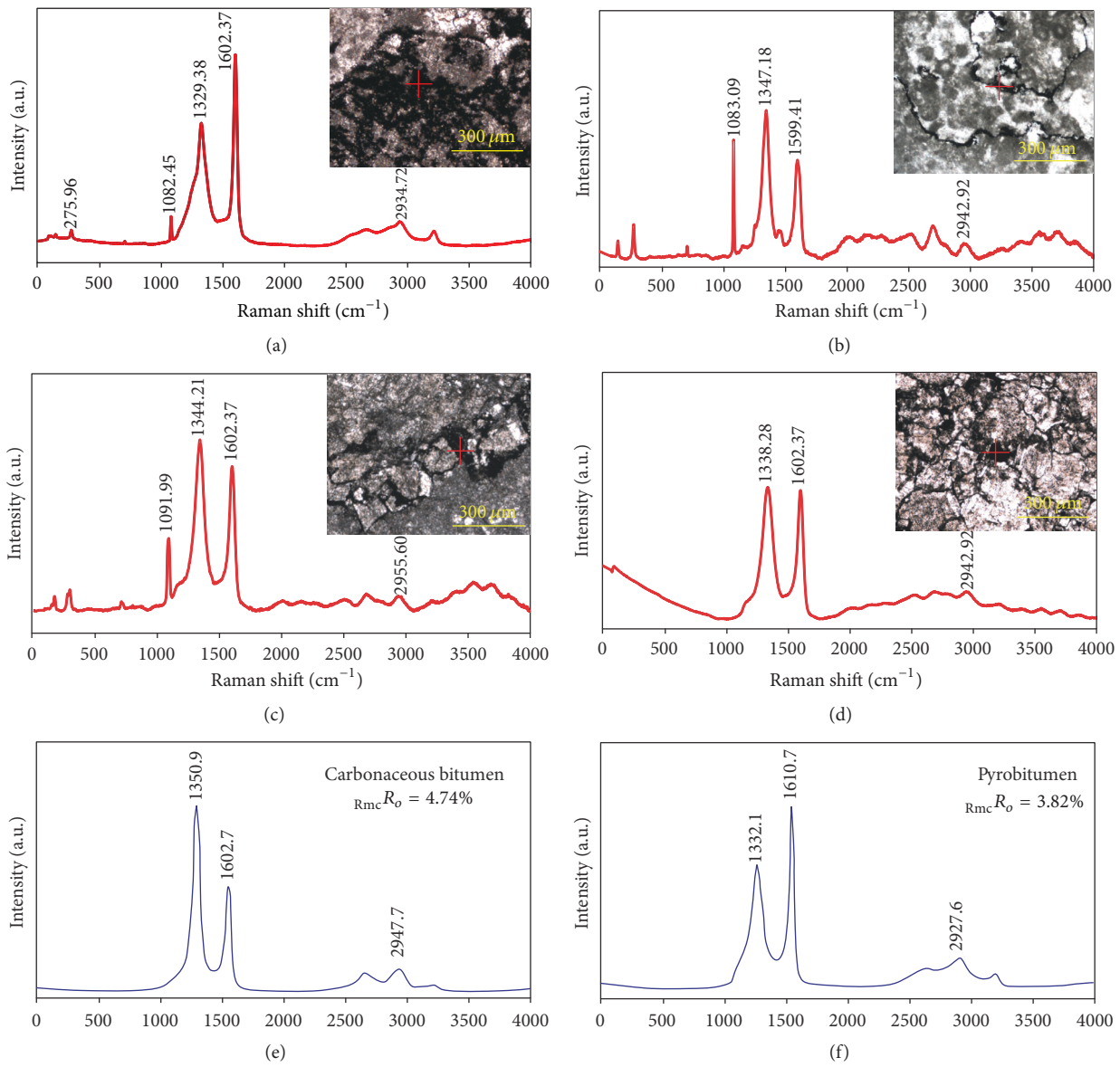

FIGURE 6: Laser Raman spectra of the solid bitumen in well DS1 and typical bitumen from previous publication. (a) DS-X06, 2864.44–2864.49 m, Rongxian Formation, oolitic limestones, 5x (−). (b) DS-X44, 4211.21 m, 1st section of Donggangling Formation, algal mudstone, 10x (−). (c) DS-X51, 4648.27 m, Yingtang Formation, algal mudstone, 5x (−). (d) DS-X53, 4648.76–4648.81 m, Yingtang Formation, dolomite, 5x (−). (e) Carbonaceous bitumen with $_{\text{Rmc}}R_o$ = 4.74% and (f) pyrobitumen with $_{\text{Rmc}}R_o$ = 3.82% taken from Liu et al. [18]. +: the exact location of the laser Raman analysis.

of aliphatic chain located in 2800–3000 cm^{-1} exist on the FTIR spectrum (Figure 8). Except for the slight absorption peak near 875 cm^{-1} and 710 cm^{-1}, the bands of out-of-plane bending vibration of C-H chemical bond have also all disappeared. It indicates that the alkyl hydrocarbon chains in the bitumen samples almost have been depleted. On the other hand, the peaks associated with aromatics C=C or C-C bonds located in 1431–1440 cm^{-1} are apparently higher than any other band peaks (Figure 8). Such characteristic FTIR spectrum generally represents the organic matter except low maturity samples, which indicates that the high thermal mature bitumen samples are enriched with aromatics and have a relatively high condensation degree of aromatic rings [4, 5, 29].

4.6. Thermal Evolution History of Devonian Carbonate Reservoirs. Based on the geothermal gradient map and the geothermal flow chart of China [43–45], the present geothermal gradient of the Guizhong Depression is about 3.5°C/100 m and the heat flux is ranging from 45 to 55 mW/m^2. According to the regional paleogeographic data, the paleogeothermal gradient in the Guizhong Depression prior to the late Indosinian uplift is estimated to be 2.82°C/100 m. There are two important uplift erosion movements in the

Table 2: Equivalent vitrinite reflectance of bitumen converted by LRM.

Sample number	Formation	Type of sample	Lithology of reservoir	Equivalent vitrinite reflectance (%)
DS-D01	D_3r	Bitumen Samples	Oolitic limestone	3.55
DS-D02				3.79
DS-D05				3.74
DS-X06				3.42
DS-X10			Algal mudstone	3.64
DS-X44	D_2d^1	Bitumen Samples	Algal mudstone	4.43
DS-X51	D_2y	Bitumen Samples	Algal mudstone	4.09
DS-X53			Dolomite	3.46
DS-X19-8-1	D_2d^1	Bitumen Inclusions	Dolomite	4.23
DS-X19-9				3.80
DS-X19-10				3.86
DS-X20-4				3.77
DS-X20-5				3.76

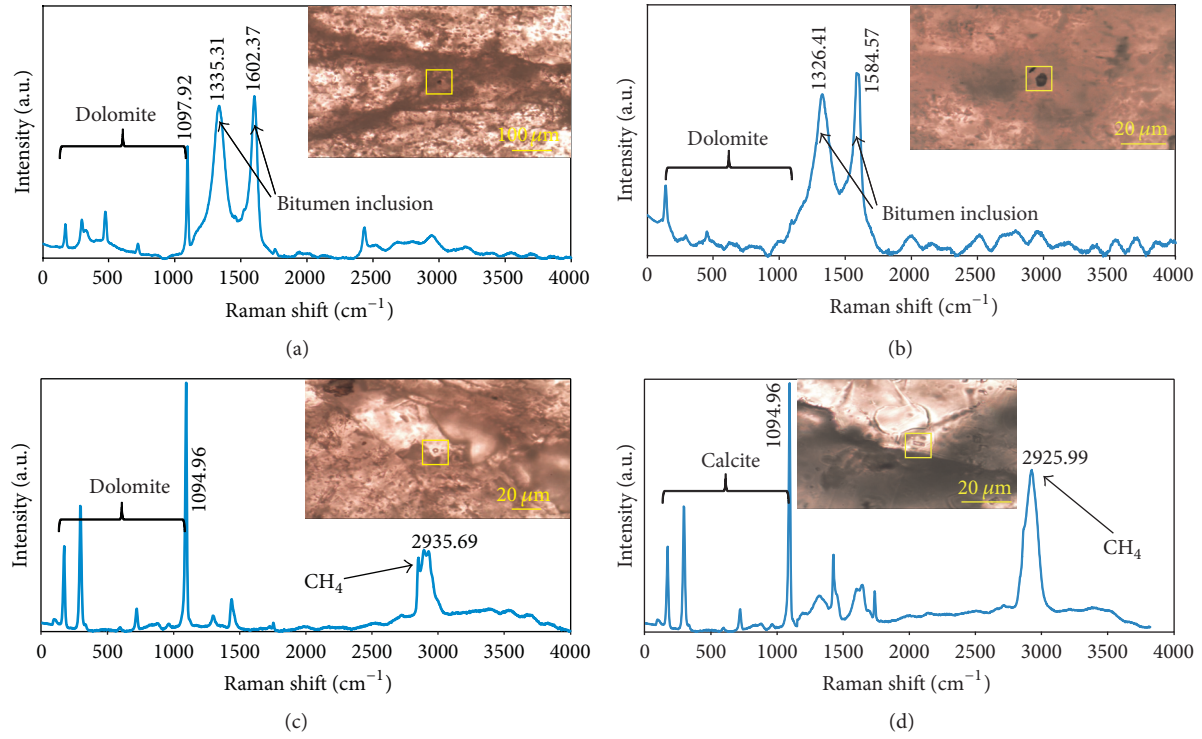

Figure 7: Laser Raman spectra for the bitumen and methane-containing fluid inclusion in the calcite vein and dolomite of well DS1. (a) DS-X19, 3894.07 m, Bitumen inclusion within the dolomite of 1st section of Dongangling Formation. ((b) and (c)) DS-X20, 3895.49 m, Bitumen and methane-containing fluid inclusion within the dolomite of 1st section of Dongangling Formation. (d) DS-X64, 4653.16 m, methane-containing fluid inclusion within the calcite vein of Yingtang Formation.

Guizhong Depression. By using the Easy% *Ro* model simplified by Wang et al. [46], the erosion thickness of the main tectonic uplift-denudation stage (late Indosinian-Yanshan-Himalayan period) in well DS1 can be restored as approximately 4012.9 m according to the measured equivalent *Ro* data in this study. The erosion thickness of the Guizhong Depression during Yanshan-Himalayan Period was calculated by the previous study to be around 4000 m based on the homogenization temperature of fluid inclusions and vitrinite reflectivity [23, 33]. The erosion thickness of Dongwu movement, which occurred during the early Indosinian, could not be calculated accurately. Its thickness roughly ranges from 300 to 500 m according to previous publications [47, 48]. In this paper, we assigned erosion thickness of 400 m for the Dongwu movement.

The detailed maturity history of Devonian carbonate reservoirs in well DS1 is modeled (Figure 9(a)). A very good correlation between measured and modeled temperatures

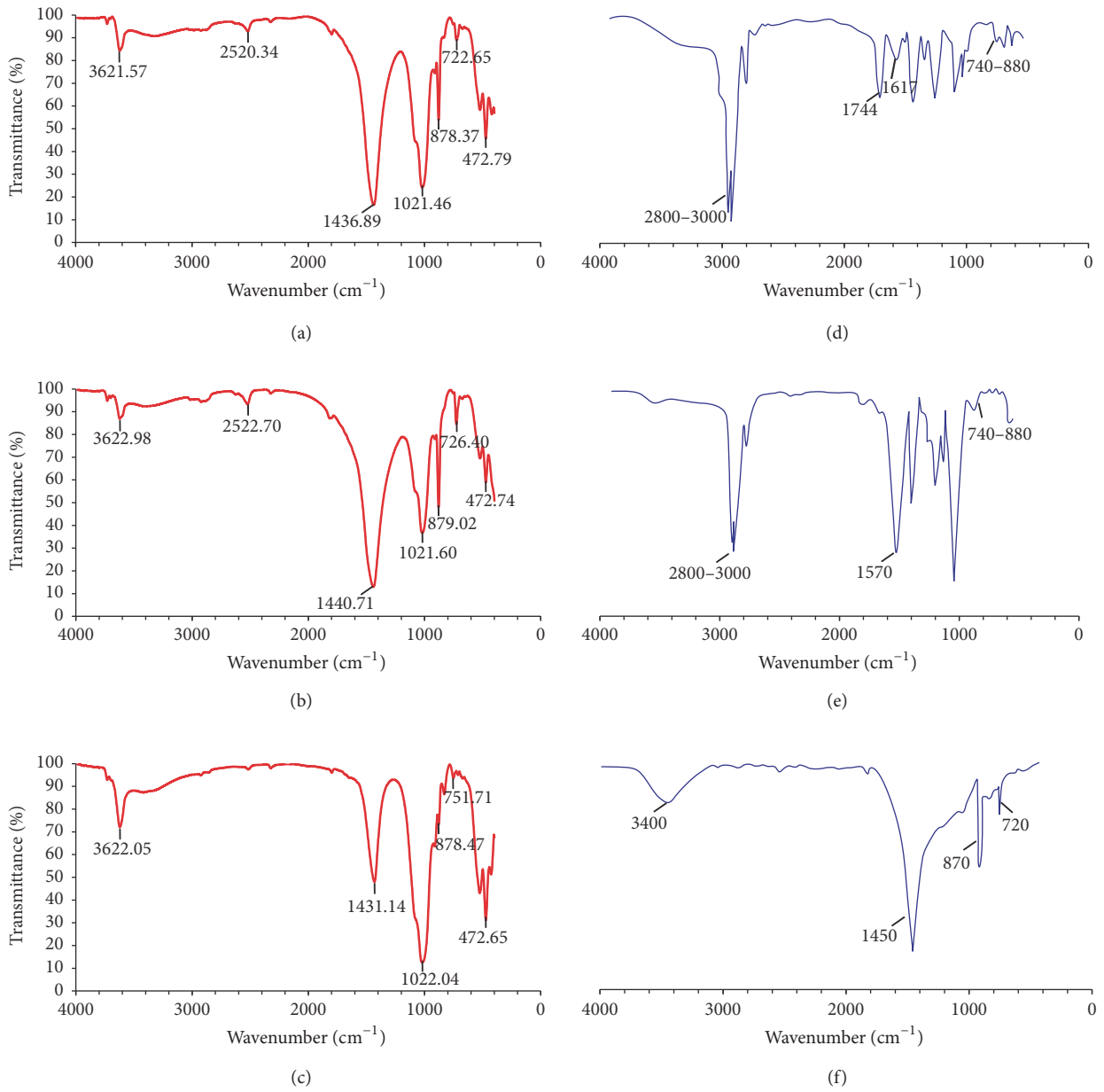

Figure 8: Infrared spectroscopy of solid bitumen in Rongxian Formation of well DS1 and other area. (a) DS-D02, 2866.70 m, (b) DS-D09, 2866.78 m, and (c) DS-D12, 2868.08 of oolitic limestone in well DS1. (d) Silurian bitumen from well H1 (6081 m) of Tarim Basin, *Ro* (%) = 0.36% [29], characterized with richness in aliphatic chains (2800–3000 cm^{-1}). (e) Carboniferous bitumen from well LN14 (5070 m) of Tarim Basin, *Ro* (%) = 0.64% [29], characterized with richness in aliphatic chains (2800–3000 cm^{-1}). (f) Cambrian bitumen from Northwestern Hunan, depth = 335 m, *Ro* (%) = 4.88% [3], characterized with lack of aliphatic chains and richness in aromatics C=C chains (1450 cm^{-1}).

and equivalent *Ro* values implies that thermal and maturity history model are a good fit for this study area (Figure 9(b)). As shown in Figure 9, the Devonian Formation began to enter early mature threshold (*Ro* = 0.5%) at a depth range of 1800–2000 m and at a temperature range of 105–115°C during the deposition of 2nd section of Dongangling Formation. Beginning at the early stage of Triassic deposition (around 240 Ma), the Devonian reservoirs passed the overmature stage threshold (*Ro* > 2.0%), successively. The maximum experienced temperature of Yingtang Formation and Rongxian Formation of well DS1 occurred during Middle Triassic and reached the highest temperature of 265°C and 225°C, respectively.

5. Discussion

5.1. Distribution Characteristics of Solid Bitumen. The fractures and the dissolution pores associated with the fracture are the main existing forms of solid bitumen in the limestone reservoirs, whereas the recrystallized pores are the main storage space for the solid bitumen in the dolomitic limestone.

There are obvious differences in the size of the ooids on both sides of the diagenetic fractures of the Upper Devonian

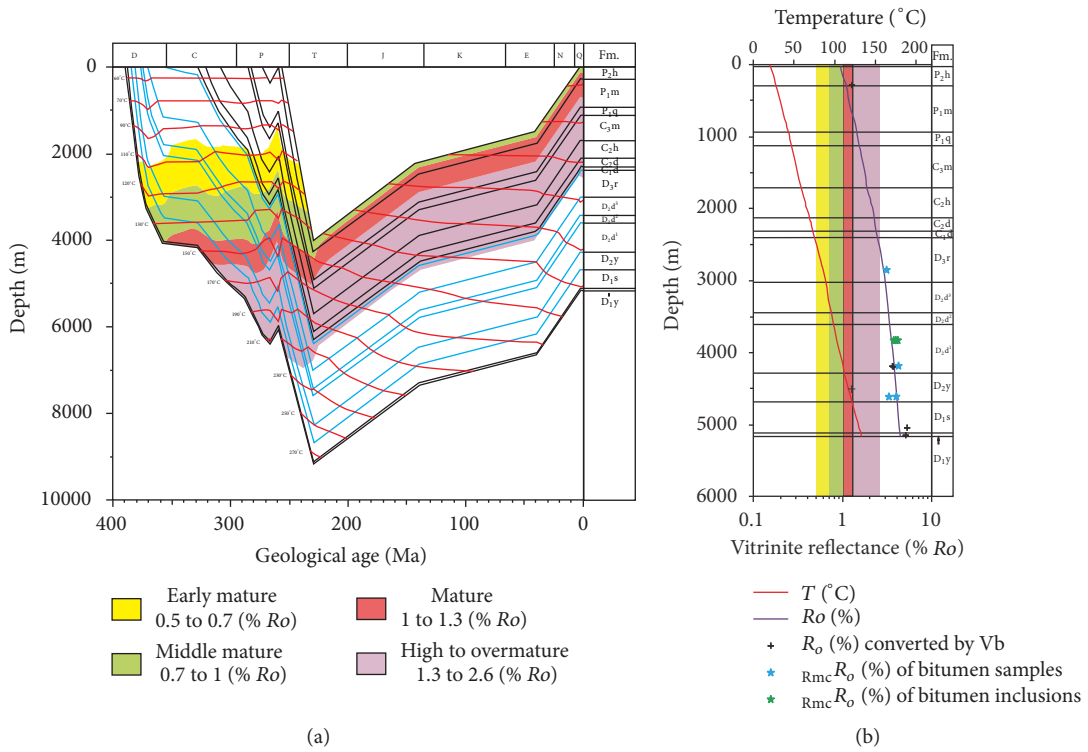

FIGURE 9: Thermal maturity history modeling of well DS1 (a) (see well location in Figure 1 and stratigraphic units in Figure 2) and temperature and maturity calibration (b) (right). +: the measured temperature (°C) and the bottom hole temperature. The red line is modelling temperature. The dark line is modelling Ro.

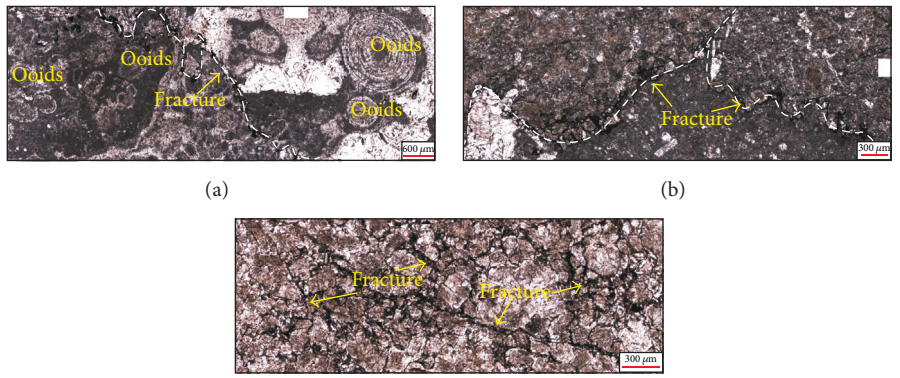

FIGURE 10: Distribution of bitumen in the carbonate reservoirs of well DS1 in Guizhong Depression. (a) DS-X08, 2866.24–2866.35 m, 5x (−), differences in ooids size on both sides of the diagenetic fracture in oolitic limestones of Rongxian Formation. (b) DS-X51, 4648.27 m, 5x (−), differences in size of calcite crystals on both sides of the dissolution fractures in algal mudstone of Yingtang Formation. (c) DS-X53, 4648.76–4648.81 m, 5x (−), grid-like dissolution fractures in dolomite of Yingtang Formation.

Rongxian Formation (Figure 10(a)), and there are also some differences in the size of calcite crystals on both sides of the diagenetic dissolved fractures (Figure 10(b)). It is speculated that these fractures are formed by mechanical compaction or tectonic stress during early diagenetic stage. These fractures were then dissolved to dissolution fractures by the liquid hydrocarbons and other acidic fluids generated at later stage. Finally, the liquid hydrocarbons were transferred into bitumen. Dissolution and recrystallization play an important role in the formation of dissolved pores and the filling of the bitumen in the dolomitic limestone of the Middle Devonian Yingtang Formation. The network distribution of the solid bitumen in the Middle Devonian Yingtang Formation indicates that it may be associated with the early developed diagenetic fractures (Figure 10(c)). The diagenetic fractures not only provide main channels for the hydrocarbons and dissolved fluids flow but also expand the distribution range of dissolution pores due to the dissolution. These crossed

fractures are favorable to bitumen and secondary calcite filling. The fractures and pores filled with solid bitumen are supposed to be formed at the early stage of oil production and injection.

In the upper section of Dongganglingformation, there is no obvious bitumen filling in the pores of high quality dolomite reservoirs. However, bitumen inclusions and methane-containing fluid inclusions found in these reservoirs could be considered as the evidences for the oil and gas activities (Figures 6 and 7). There are two possible reasons for this phenomenon: one is that the reservoirs were formed before the main period of liquid hydrocarbon generation and migration but were not in the favorable place for the hydrocarbon accumulation in the reef traps. They are only the carrier beds, even not on the main migration path for the hydrocarbons. Thus, these reservoirs only captured a small amount of hydrocarbon inclusions. The other reason could be that the reservoirs were formed after the significant hydrocarbon generation and charging. Only a small amount of hydrocarbon inclusions was captured during the hydrocarbon migration process of fluid activity after the reservoir destruction. With the same reason, there were no obvious bitumen deposits in the flat tectonic fractures of the reservoir (Figures 4(g) and 4(h)). Few inclusions of bitumen and methane were found in some calcite veins (Figure 5), indicating that these fractures probably formed during the adjustment and reform stage of liquid hydrocarbon accumulation.

5.2. Thermal Maturity of Solid Bitumen. The bitumen observed on the core DS1 was described as hard, brittle, steel-gray, insoluble in chloroform, conchoidal fracture, and nonfluorescent. These features are similar to the carbon bitumen with high thermal evolution degree in paleoreservoirs of Nanpanjiang area [1, 24]. This suspected solid bitumen observed by microscope mainly filled in the microfractures, intergranular pores, dissolved holes, and intercrystal pores and display several regular morphologies (Figure 4). They show some clear characteristics of pyrobitumen and similar to the solid bitumen in the carbonate reservoir of well Guizhong 1, Sichuan Basin [1, 49]. This pyrobitumen is different from the precipitation bitumen and biodegraded bitumen which are grainy and irregular in shape.

The spectra of the laser Raman spectroscopy and infrared spectroscopy suggest that the solid bitumen has characteristics of highly evolved aromatic compounds. The vitrinite reflectances calculated by the laser Raman spectra are strongly consistent with the vitrinite reflectances converted from bitumen reflectance (Tables 1 and 2), indicating that the solid bitumen has reached a mature stage of metamorphism. In order to highlight the high thermal maturity characteristics of the solid bitumen in this study, the infrared spectra of the solid bitumen in Rongxian Formation are compared with the different maturity bitumen published by previous researchers (Figure 8). The infrared spectroscopy of the low maturity bitumen from Tarim Basin is characterized as aliphatic chains enrichment (2800–3000 cm^{-1}) (Figures 8(d) and 8(e)), which is obviously different from the solid bitumen in this study [4, 29]. The solid bitumen of Rongxian Formation is similar to the anthraxolite of Cambrian (*Ro*% is 4.88%) reported by Cao et al. [3], which is characterized with lack of aliphatic chains but richness in aromatics C=C chains (1450 cm^{-1}). The result of comparison demonstrates that the solid bitumen had undergone a very high thermal evolution degree and had evolved to the residual carbonaceous stage such as pyrobitumen and schungite [2, 5].

5.3. Thermal Evolution History of Devonian Reservoirs. According to the comprehensive analysis of basin simulation and the thermal maturity of solid bitumen, the thermal evolution history of Devonian reservoirs in well DS1 can be divided into four stages:

(1) The early rapid burial-warming stage from Early and Middle Devonian to Middle and Late Permian: the Rongxian Formation entered the medium mature stage and the bottom temperature of the reservoir reached 140°C. The 1st sections of Dongganglingformation and the Yingtang Formation were in stage of mature to overmature, and the temperature of the reservoir reached up to 190°C. After this stage, the liquid crude oil that filled the Devonian carbonate reservoir has been cracked into wet gas and lower maturity bitumen.

(2) During the Late Permian, the study area entered into a temporary uplift-cooling stage caused by Dongwu movement. The Devonian reservoir was uplifted several hundred meters, and the reservoir temperature decreased by about 10–20°C.

(3) The rapid burial-warming stage from Late Permian to Early and Middle Triassic: at the end of the Permian, the 1st section of Dongganglingformation and the Yingtang Formation completely entered the overmature stage, and the temperature of the reservoirs was over 200°C. The lower part of Rongxian Formation also entered into overmature stage at Early Triassic (*Ro* = 2.0%). As a result of this rapid burial and warming up, the entire Devonian reservoirs in well DS1 have experienced the stage of overmature and metamorphism. And they have reached the highest reservoir temperature of 210–260°C before the tectonic uplift caused by late Indosinian orogeny occurred at the late period of Early Triassic. At this stage, the lower maturity bitumen was further thermally cracked into pyrobitumen because of high temperature.

(4) Since Middle Triassic, the study area entered a slow uplift and cooling stage. The uplift and erosion that occurred during Yanshan-Himalayan period have significant influence on the thermal maturity evolution of the Devonian reservoirs. From 230Ma to present, there was no increase in the maturity probably because of the uplift and having no deeper burial. The temperature of Devonian reservoirs has been reduced by 120°C due to the uplift to the present-day depth.

6. Conclusions

The following conclusions can be drawn in this study:

(1) Fractures and fracture-related dissolution pores are the main storage space for solid bitumen.

(2) The equivalent vitrinite reflectance of the solid bitumen in well DS1 ranges from 3.42% to 4.43%, and no aliphatic chains were detected by the FTIR.

(3) The pyrobitumen in Devonian carbonate reservoir is supposed to be the result of thermal cracking in the high temperature after crude oil charged into the reservoir at the early stage.

(4) The thermal maturity history demonstrates that the Devonian reservoirs have experienced four stages. The entire Devonian reservoirs reached the highest reservoir temperature 210–260°C during the second rapid burial-warming stage, which is the main period for solid bitumen formation.

Conflicts of Interest

The authors declare that they have no conflicts of interest.

Acknowledgments

The study was financially supported by the National Science Foundation of China (no. 41302111; no. 41672139), the Program of Introducing Talents of Discipline to Universities (no. B14031), the Foundation of China Geological Survey (no. 12120114046901), and the thirteenth research plan of the Ministry of Science and Technology of China (nos. 2016ZX05034002-003 and 2017ZX05049005-007). The authors are very grateful to the Petroleum Exploration Branch Company of Sinopec for their kind help and support to complete this study and the permission to publish the results.

References

[1] M. Zhao, S. Zhang, L. Zhao, and J. Da, "Geochemical features and genesis of the natural gas and bitumen in paleo-oil reservoirs of Nanpanjiang Basin, China," *Science in China, Series D: Earth Sciences*, vol. 50, no. 5, pp. 689–701, 2007.

[2] W. G. Li, Y. H. Duan, L. K. Yan, and Z. Z. Sun, "Study on measuring method of asphalt using infrared spectrum characteristic of petroleum pitch," *Petroleum Asphalt*, vol. 26, pp. 9–14, 2012 (Chinese).

[3] D. Y. Cao, X. S. Zhu, J. M. Deng, Z. N. Li, and Y. D. Wu, "Analysis on features of anthraxolite from Northwestern Hunan Wanrongjiang Mine and geological meaning," *Coal Science and Technology*, vol. 41, pp. 109–112, 2013.

[4] T. S. Song, L. Liu, Q. A. Meng, N. Liu, and X. R. Ming, "Characteristics of reservoir bitumen and its influence on reservoir properties in Fuyu oil layer, Daqing Placanticline," *Global geology*, vol. 34, pp. 1079–1083, 2015 (Chinese).

[5] R. H. Zhang, C. S. Si, L. Huang et al., "Genesis and evolution of reservoir bitumen in Xiaocaoba paleo-oil reservoir, Qianbei Depression," *Peteoleum Geology & Experiment*, vol. 39, pp. 99–105, 2017 (Chinese).

[6] Y. Xiong, W. Jiang, X. Wang et al., "Formation and evolution of solid bitumen during oil cracking," *Marine and Petroleum Geology*, vol. 78, pp. 70–75, 2016.

[7] A. J. Lomando, "The influence of solid reservoir bitumen on reservoir quality," *AAPG Bull*, vol. 76, pp. 1137–1152, 1992.

[8] L. F. Liu, J. Z. Zhao, S. C. Zhang, J. H. Fang, and Z. Y. Xiao, "Genetic types and characteristics of the Silurian asphaltic sandstones in Tarim Basin," *Acta Petrolei Sinica*, vol. 21, no. 6, pp. 12–17, 2000 (Chinese).

[9] J. C. Jin, J. Z. Qin, Z. R. Zhang, M. Fan, and Q. Zhang, "Genetic analysis of the high maturated bitumen in Songpan-Aba area," *Petroleum Geology & Expeximent*, vol. 26, no. 4, pp. 370–374, 2004.

[10] Rogers, "Significance of reservoir bitumens to thermal maturation studies, Western Canada Basin," *AAPG*, vol. 58, no. 9, pp. 1806–1824, 1974.

[11] L. D. Stasiuk, "The origin of pyrobitumens in Upper Devonian Leduc Formation gas reservoirs, Alberta, Canada: An optical and EDS study of oil to gas transformation," *Marine and Petroleum Geology*, vol. 14, no. 7-8, pp. 915–929, 1997.

[12] R. J. Hwang, S. C. Teerman, and R. M. Carlson, "Geochemical comparison of reservoir solid bitumens with diverse origins," *Organic Geochemistry*, vol. 29, no. 1-3, pp. 505–517, 1998.

[13] S. R. Kelemen and H. L. Fang, "Maturity trends in Raman spectra from kerogen and coal," *Energy and Fuels*, vol. 15, no. 3, pp. 653–658, 2001.

[14] Y. Zeng and C. Wu, "Raman and infrared spectroscopic study of kerogen treated at elevated temperatures and pressures," *Fuel*, vol. 86, no. 7-8, pp. 1192–1200, 2007.

[15] J. J. Sweeney and A. K. Burnham, "Evolution of a simple modal of vitrite reflectance on chemical kinetics," *AAPG Bull*, vol. 74, pp. 1559–1570, 1990.

[16] J. W. Schopf, A. B. Kudryavtsev, D. G. Agresti, A. D. Czaja, and T. J. Wdowiak, "Raman imagery: A new approach to assess the geochemical maturity and biogenicity of permineralized Precambrian fossils," *Astrobiology*, vol. 5, no. 3, pp. 333–371, 2005.

[17] J. W. Schopf and A. B. Kudryavtsev, "Confocal laser scanning microscopy and Raman imagery of ancient microscopic fossils," *Precambrian Research*, vol. 173, no. 1-4, pp. 39–49, 2009.

[18] D. Liu, X. Xiao, H. Tian et al., "Sample maturation calculated using Raman spectroscopic parameters for solid organics: Methodology and geological applications," *Chinese Science Bulletin*, vol. 58, no. 11, pp. 1285–1298, 2013.

[19] L. Wei, Y. Wang, and M. Mastalerz, "Comparative optical properties of macerals and statistical evaluation of mis-identification of vitrinite and solid bitumen from early mature Middle Devonian – Lower Mississippian New Albany Shale: Implications for thermal maturity assessment," *International Journal of Coal Geology*, vol. 168, pp. 222–236, 2016.

[20] A. Grobe, J. L. Urai, R. Littke, and N. K. Lünsdorf, "Hydrocarbon generation and migration under a large overthrust: The carbonate platform under the Semail Ophiolite, Jebel Akhdar, Oman," *International Journal of Coal Geology*, vol. 168, pp. 3–19, 2016.

[21] H. D. Chen, M. C. Hou, W. J. Liu, and J. C. Tian, "Basin evolution and sequence stratigraphic framework of south of China during Hercynian cycle to Indo-Chinese epoch," *Journal of Chengdu University of Technology: Science & Technology Edition*, vol. 31, no. 6, pp. 629–635, 2004 (Chinese).

[22] M. C. Hou, H. D. Chen, and J. C. Tian, "Study on reservoir characteristics of the Late Paleozoic reef in Youjiang basin, China," *Journal of Chendu University of Technolegy (Science & Technology Edition)*, vol. 32, no. 3, pp. 231–238, 2005 (Chinese).

[23] Z. L. Chen, G. S. Yao, Q. X. Guo et al., "Hydrocarbon accumulation and thermal reconstruction of Neopaleozoic marine strata in Guizhong Depression," *Marine Origin Petroleum Geology*, vol. 15, no. 3, pp. 1–10, 2010 (Chinese).

[24] X. Y. He, G. S. Yao, X. S. He et al., "Bitumen genesis and hydrocarbon accumulation pattern of Well Guizhong-1 in Guizhong Depression," *Acta Petrolei Sinica*, vol. 31, no. 3, pp. 420–431, 2010 (Chinese).

[25] L. Huang, Z. Y. Xu, P. W. Wang, and S. Y. Xiong, "An analysis of resource potential of Upper Paleozoic shale gas in Guizhong depression," *Geology in China*, vol. 39, no. 2, pp. 497–506, 2012 (Chinese).

[26] P. W. Wang, G. S. Yao, Z. L. Chen et al., "Characteristics and evolution of Devonian reef reservoirs in Guizhong (central Guangxi) depression," *Geology in China*, vol. 38, no. 1, pp. 170–179, 2011 (Chinese).

[27] S. G. Liu and Z. L. Luo, "Study on the distribution characteristics of petroleum deposits from the plate tectonic evolution in South China," *Acta Petrolei Sinica*, vol. 22, no. 4, pp. 24–30, 2001 (Chinese).

[28] M. J. Zhao, S. C. Zhang, and L. Zhao, "Geochemistry and genesis of bitumen in paleo-oil reservoir in the Nanpanjiang Basin, China," *Acta Geologica Sinica*, vol. 80, pp. 893–901, 2006.

[29] D. M. Liu, K. L. Jin, H. L. Mao, W. M. Du, and Hu. J. Study of, "Study of macerals in hydrocarbon source rocks by fourier transform infrared microspectroscopy," *Acta Petrologica Sinica*, vol. 14, pp. 222–231, 1998 (Chinese).

[30] Z. C. Mao, Y. S. Du, M. Zhang, J. X. Yan, and F. Zeng, "Organic geochemical characterization and depositional paleoenvironments of the Devonian strata in Guizhong region, Guangxi, China," *Science in China, Series D: Earth Sciences*, vol. 52, no. 1, pp. 88–95, 2010.

[31] J. W. Kang, X. B. Lin, J. C. Tian, and X. Zhang, "Reservoir characteristics within the Devonian sequence stratigraphic framework in the southern Guizhou-central Guangxi region," *Sedimentary Geology and Teheyan Geology*, vol. 30, pp. 76–83, 2010.

[32] L. X. Fu, P. Yu, S. L. Li, Q. J. Zhang, and Y. Gao, "Prediction of devonian reef distribution in guizhong deperssion," *Marine Origin Petroleum Geology*, vol. 14, pp. 35–41, 2009 (Chinese).

[33] Z. H. Lou, C. J. Shang, G. S. Yao, Z. L. Chen, and A. M. Jin, "Hydrocarbon preservation conditions in marine strata of the Guizhong depression and its margin," *Acta Petrolei Sinica*, vol. 32, no. 3, pp. 432–441, 2011 (Chinese).

[34] H. Jacob, "Classification, structure, genesis and practical importance of natural solid oil bitumen ("migrabitumen")," *International Journal of Coal Geology*, vol. 11, no. 1, pp. 65–79, 1989.

[35] G. X. Feng and S. J. Chen, "Relationship between the reflectance of bitumen and vitrinite in rock," *Nature Gas Industry*, vol. 8, no. 3, pp. 20–25, 1988.

[36] D. H. Liu and J. Y. Shi, "Discussion on unconventional evaluation method of high maturated carbonate source rock," *Petroleum Exploration and Development*, vol. 21, no. 3, pp. 113–115, 1994.

[37] B. P. Tissot and D. H. Welte, *Petroleum Formation and Occurrence*, Springer, Berlin, Germany, 2nd edition, 1984.

[38] P. A. Allen and J. R. Allen, *Basin Analysis: Principles and Application*, Blackwell Scientific Publications, Oxford, England, 1990.

[39] J. M. Hunt, *Petroleum Geochemistry and Geology*, Springer, Berlin, Germany, 1996.

[40] H. Ganz and W. Kalkreuth, "Application of infrared spectroscopy to the classification of kerogentypes and the evaluation of source rock and oil shale potentials," *Fuel*, vol. 66, no. 5, pp. 708–711, 1987.

[41] S. R. Dalal, S. K. Menon, and Y. K. Agrawal, "Infrared spectroscopic studies of EOM from Cambay Basin," *Journal of the Indian Chemical Society*, vol. 73, pp. 247–253, 1996.

[42] A. A. Christy, B. Dahl, and O. M. Kvalheim, "Structural features of resins, asphaltenes and kerogen studied by diffuse reflectance infrared spectroscopy," *Fuel*, vol. 68, no. 4, pp. 430–435, 1989.

[43] E. X. Jiang, "Terrestrial heat flow pattern and thermo-tectonic domains in continental area of China," *Journal of the Graduate School of the Chinese Academy of Sciences*, vol. 18, no. 1, pp. 51–58, 2001 (Chinese).

[44] S. B. Hu, L. J. He, and J. Y. Wang, "Compilation of heat flow data in the China continental area (3rd edition)," *Chinese Journal of Geophysics*, vol. 44, no. 5, pp. 611–626, 2001 (Chinese).

[45] Y. S. Yuan, Y. S. Ma, S. B. Hu, T. L. Guo, and X. Y. Fu, "Present-day geothermal characteristics in South China," *Chinese Journal Geophysics*, vol. 49, no. 4, pp. 1118–1126, 2006 (Chinese).

[46] W. Wang, Z. Zhou, and P. Yu, "Relations between vitrinite reflectance, peak temperature and its neighboring thmperature variation rate: a comparison of methods," *Chinese Journal Geophysics*, vol. 48, no. 6, pp. 1375–1386, 2005 (Chinese).

[47] B. He, Y. G. Xu, Y. M. Wang, and L. Xiao, "Nature of the Dongwu movement and its temporal and spatial evolution," *Earth Science — Journal of China University of Geosciences*, vol. 30, pp. 89–96, 2005 (Chinese).

[48] C. Q. Zhu, M. Xu, J. N. Shan, Y. S. Yuan, Y. Q. Zhao, and S. B. Hu, "Quantifying the denudations of major tectonic events in Sichuan basin: Constrained by the paleothermal records," *Geology in China*, vol. 36, pp. 1268–1277, 2009 (Chinese).

[49] S. Z. Hu, S. F. Li, X. W. Fu, Y. J. Li, and T. D. Wang, "Identification of highly to over mature gas interval using reservoir bitumen features: Sichuan basin of Southwest China," *Petroleum Science and Technology*, vol. 32, no. 12, pp. 1437–1442, 2014.